

Structural Properties of Amorphous $\text{Al}_2\text{O}_3\cdot 2\text{SiO}_2$ nanoparticles

Nguyen Ngoc Linh*, Vo Van Hoang* and Hoang Zung**

*Dept. of Physics, Institute of Technology, National Univ. of HochiMinh City,
268 Ly Thuong Kiet Str., Distr. 10, HochiMinh City, Vietnam, ngoclinh84phys@yahoo.com

**Dept. of Science and Technology, National Univ. of HochiMinh City, Vietnam

ABSTRACT

Structural properties of amorphous $\text{Al}_2\text{O}_3\cdot 2\text{SiO}_2$ (denoted as AS_2) spherical nanoparticles have been studied in a model with different sizes of 2 nm, 3 nm and 4 nm under non-periodic boundary conditions with the Born-Mayer type pair potentials via molecular dynamics (MD) simulation. Structural properties were studied in details through the partial radial distribution functions (PRDF), coordination number distribution, bond-angle distributions and interatomic distances. Moreover, the radial density profiles in nanoparticles were also obtained. Calculations show that size effects on structure of a model are significant and calculated data differ from those obtained previously in the bulk one. We find that as the size larger than 3 nm, amorphous AS_2 nanoparticle has a distorted tetrahedral network structure with the mean coordination number $Z_{\text{Al-O}} \approx 4$ and $Z_{\text{Si-O}} \approx 4$. The existence of triclusters in nanoparticles and size dependence of tricluster composition have been found and discussed. Furthermore, surface structure and surface energy of nanoparticles have been obtained and presented.

Keywords: amorphous aluminosilicate, nanoparticles.

1 INTRODUCTION

Aluminosilicate nanoparticles have been interested for many years because of their important technical applications in biomedicine, optics and electronics, etc. [1-3]. In particular, in oil industry aluminosilicate nanoparticles containing 9.0-20 nm mesopores were prepared for cracking of very large hydrocarbon [4-5]. Therefore, it is also of fundamental importance to understand their properties. In recent years, the amorphous AS_2 materials on the nanoscale have been synthesized and studied by different experiments such as x-ray scattering, dynamic light NMR spectroscopy, and differential thermal analysis [6-8]. In addition, research of structure of aluminosilicate nanoparticles by force field calculations on extended systems and ab initio quantum chemical calculations on ring structures was carried out [9]. However, more detailed information about local structure of amorphous AS_2 nanoparticles have not been investigated yet. In contrast, these properties of aluminosilicate bulk materials have been under intensive investigations by both

experiments and numerical methods [10-17]. On other hand, according to our previous work, it was found that liquid and amorphous bulk AS_2 have relatively large amount of five-and six-fold coordinated Al atoms in addition to AlO_4 units [15-16] and agrees well with experiments [10-11]. Therefore, it motivates us to carry out the systematic analysis of structure of amorphous AS_2 nanoparticles compared with those observed in the bulk. In addition, evolution of surface effects with different sizes has been observed and presented.

2 CALCULATION

The simulations were done in a spherical particle under non-periodic boundary conditions with the sizes of 2nm, 3nm and 4nm, which contains the number of atoms corresponding the real density of $2.6 \text{ g}\cdot\text{cm}^{-3}$ for amorphous AS_2 [17]. The interatomic potentials of the Born-Mayer type which were successfully used in our previous works for liquid and amorphous $\text{Al}_2\text{O}_3\cdot 2\text{SiO}_2$ [15-16] and their form is given below:

$$U_{ij} = Z_i Z_j \frac{e^2}{r} + B_{ij} \exp\left(-\frac{r}{R}\right) \quad (1)$$

Where the terms present Comlomb and repulsion energies, respectively. Here r denotes the distances between the centers of i th and j th ions: $Z_{\text{Al}} = +3$, $Z_{\text{Si}} = +4$, $Z_{\text{O}} = -2$; B_{ij} and R_{ij} are the parameters accounting for the repulsion of the ionic shells. The values $B_{\text{AlAl}} = 0$, $B_{\text{AlSi}} = 0$, $B_{\text{SiSi}} = 0$, $B_{\text{AlO}} = 1779.89 \text{ eV}$, $B_{\text{SiO}} = 1729.50 \text{ eV}$, $B_{\text{OO}} = 1500 \text{ eV}$, and $R_{ij} = 29 \text{ pm}$. More details about these potentials can be found in Refs. [15,16,18]. Comlomb interactions were taken into account by mean of Ewald-Hansen method and the Verlet algorithm with the MD time step 1.6 fs. We first placed randomly N atoms in a sphere of fixed radius and the configuration has been relaxed for 50000 MD steps at 7000 K, after that the systems were cooling down linearly in the time from the melt at constant volume to the temperature of 350 K with cooling rate $\gamma = 4.375 \times 10^{13} \text{ K}\cdot\text{s}^{-1}$. Structural quantities have been calculated similarly as it was done for the bulk one after relaxing for 80 ps at this temperature [16].

Table 1: Structural characteristics of amorphous AS₂ at 350K; R_{ij} - position of the first peaks in PDRFs; Z_{ij} - the average coordination number.

Materials	R _{ij} (Å)						Z _{ij}			
	Al-Al	Al-Si	Si-Si-	Al-O	Si-O	O-O	Al-O	O-Al	Si-O	O-Si
2 nm	3.19	3.14	3.09	1.62	1.50	2.50	3.77	1.51	4.05	1.36
3 nm	3.20	3.12	3.08	1.64	1.50	2.50	4.01	1.61	4.03	1.35
4 nm	3.19	3.14	3.08	1.64	1.50	2.50	4.10	1.67	4.08	1.39
Amorphous bulk models [16]	3.17	3.16	3.09	1.72	1.51	2.50	4.57	1.30	4.18	1.19
Exp. for the amorphous bulk [12-14]				1.71			4.54		~4	
				1.77						

3 RESULTS AND DISCUSSIONS

In order to obtain the size dependence of structure of amorphous AS₂ nanoparticles, in this work we show the structural characteristics of well-relaxed models at 350 K.

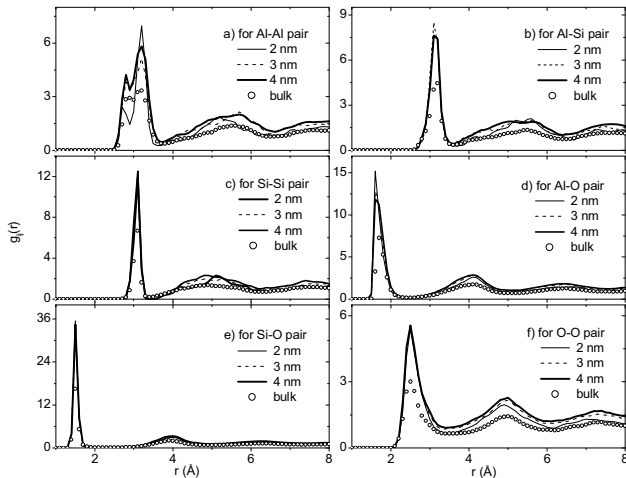


Fig. 1: Radial distribution functions of amorphous AS₂ nanoparticles and bulk [16] at 350 K.

The first quantity we would like to discuss here is the PRDF for different atomic pairs. As shown in Fig. 1 and Table 1, we can see that the position of the first peaks in PRDFs changes slightly with particles size and it has smaller value compared with those for the bulk one with an exception Al-Al pair. The peaks in PRDF of nanoparticles are boarder and higher than that for the bulk one indicated that the structure of amorphous nanoparticle is more heterogeneous than that for the bulk one due to the contribution of surface structure of formers [19]. It is essential to notice that PRDF for the Al-Al pair of nanoparticles is also splitting into two peaks at the near positions like those observed in the bulk one. It means that in network structure of amorphous AS₂ nanoparticles, there are two different characteristic length scales r_1 and r_2 for distance between nearest Al neighbors. These two scales

should be also reflected in the geometry of the AlO₄ tetrahedra and two connected tetrahedra for which the Al atoms are located at a distance r_1 from each other may have a different geometry from two connected tetrahedra where the two Al atoms in the centre are at distance of around r_2 . It may be related to the existence of small-membered rings like those discussed in [17].

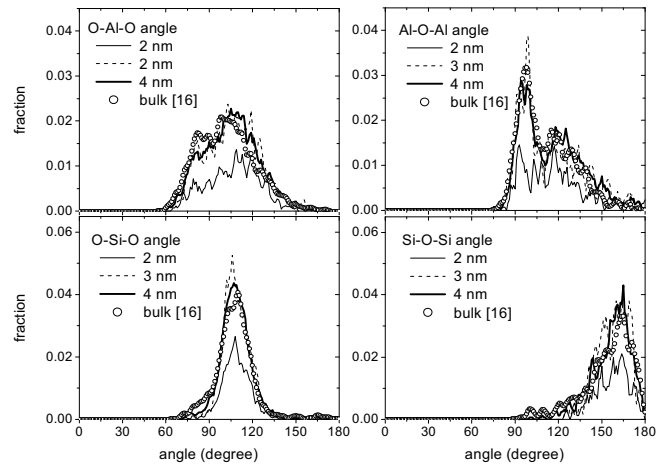


Fig. 2: Bond-angle distributions in amorphous AS₂ nanoparticles.

As discussed in previous simulations and experiments [12,15], the larger values obtained for Al-O bond lengths are in accordance to a distorted tetrahedral network structure in amorphous AS₂ bulk model because it is related to the large number of over-coordinated structural units such as AlO₅ and AlO₆ in the bulk one (i.e. $Al^V-O=1.83 \text{ \AA}$, $Al^{VI}-O=1.88 \text{ \AA}$) [12-13]. The mean coordination number for Al-O and Si-O pairs in amorphous nanoparticles, however, is lower than that for the bulk one and it is more close to those for ideal tetrahedral coordinated Al-O and Si-O network [18,20]. In contrast, for O-Al and O-Si it increases with increasing of nanoparticle sizes and larger than those for the bulk one. One can see clearly this tendency via the mean coordination numbers for different

atomic pairs presented in Table 1. It indicates the changes of tricluster distributions in structure of amorphous AS₂ nanoparticles. Like those obtained for the bulk one [16], i.e. it was found that about approximate 43% oxygen atoms are three-fold coordinated by (Al, Si) atoms. In the amorphous AS₂ nanoparticles, percentage of the O atoms with three-fold coordinated by (Si, Al) atoms is equal to 25%, 28% and 31% for the sizes of 2nm, 3nm and 4nm, respectively. The details of cation compositions of the triclusters are shown in Table 2. Moreover, information about local structure of nanoparticles can be found via the most important bond-angle distributions such as O-Al-O, Al-O-Al, and analogously O-Si-O and Si-O-Si angles. From Fig. 2, we can see that such distributions also depend on the size of particles due to the surface effects. For particle with the size of 3 nm and 4 nm the main peak of distribution for O-Al-O angle is at 105.3° which is close with that for O-Si-O angle, i.e. 106°, and close with those for the tetrahedral network structure. In contrast, for Al-O-Al angle is at around 94.3° and is much less than that of Si-O-Si angle which is equal to 165°. This indicates that the packing of AlO_x units in the AS₂ system is denser than those of SiO_x units. On other hand, the main peaks in distribution for the angles are located at around the values close to those for ideal tetrahedra [18,20], like those discussed above. Another important structural quantity of nanoparticle is the dependence of particle density $\rho(R)$ on the distance R from the center of nanoparticle. In addition, it fluctuates around the real density of amorphous AS₂ of 2.6 g.cm⁻³ of amorphous material. However, it increases up to 3.0 g.cm⁻³ at layer around surface. One can see clearly such change via the radial density profile for amorphous AS₂ nanoparticles with the size of 4 nm in Fig. 3. Furthermore, in order to gain more insights of surface structure for nanoparticles we show the partial atomic density profiles for Al, Si and O atoms separately in Fig. 4. At surface layer of amorphous AS₂ nanoparticles, we can see that O atoms have tendency to concentrate at the surface of nanoparticles like those observed in amorphous SiO₂ clusters [19]. The reason for such phenomenon is that the system is energetically better to O atoms at the surface because only one bond has to be broken and Al atoms, $Z_{Al} = +3$, also have a tendency to

concentrate at the surface together with O ones for partial charge neutrality, whereas if a Si atom, $Z_{Si} = +4$, is at the surface, several bonds have to be broken. And due to the excess of O at the surface, Si atoms have a tendency to concentrate in the layer just below the surface for local charge neutrality. However, in Figs. 3 and 4 these profiles fluctuate strongly, which indicate that our statistics are not good, smoother changes of the curves can be obtained via averaging over many independent runs. Moreover, in order to clarify structural changes in nanoparticles with different sizes, we show the mean coordination number for different atomic pairs in the core and in the 3.19 Å top spherical shells of nanoparticles (Table 3). Structural properties of surface and core strongly depend on the size of nanoparticles. First, in the surface shells, the mean coordination number for different atomic pairs increases with increasing of size with an exception for Z_{Si-O} . The surface mean coordination number for Si-O pairs decreases from 4.05 to 4.01 and these values are close with those for an ideal tetrahedron. In contrast, for Al-O pairs it is much smaller than the value of 4.00, which indicates a larger number of under-coordinated Al atoms in surface layer of amorphous AS₂ nanoparticles. The mean coordination number for the Al-O and Si-O pairs in the core of nanoparticles is larger than that in the surface layer and is around the value of 4.00. Moreover, mean coordination number for other atomic pairs in the core of nanoparticles is also higher than those in the surface layer indicated the differences of structure of the core and surface of nanoparticles.

Table 2: Composition of triclusters.

Material	Number of Al atoms in triclusters			
	0	1	2	3
2nm	0 %	9 %	60.2 %	30.8 %
3nm	0.5 %	9.4 %	55.3 %	34.8 %
4nm	0.4 %	10.2 %	56.5 %	32.9 %
Bulk [16]	1.1 %	16.2 %	56.8 %	25.9 %

Table 3: The mean coordination number in the surface shell and in the core of nanoparticles at the temperature of 350 K.

Materials		Z_{Al-Al}	Z_{Al-Si}	Z_{Si-Al}	Z_{Si-Si}	Z_{Al-O}	Z_{O-Al}	Z_{Si-O}	Z_{O-Si}	Z_{O-O}
2nm	Surface	2.53	2.25	2.45	2.12	3.48	1.40	4.05	1.36	6.85
	Core	3.70	3.00	3.13	2.33	4.35	1.79	4.06	1.34	8.83
3nm	Surface	2.20	2.35	2.38	2.13	3.51	1.34	4.01	1.37	6.92
	Core	4.00	2.82	3.06	2.39	4.38	1.84	4.08	1.34	9.47
4nm	Surface	2.87	2.31	2.54	2.13	3.68	1.46	4.01	1.37	7.15
	Core	3.81	2.95	3.04	2.44	4.00	1.78	4.09	1.37	9.39

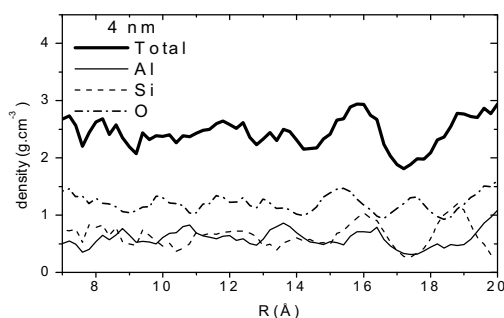


Fig. 3: Density profile in amorphous AS₂ nanoparticles.

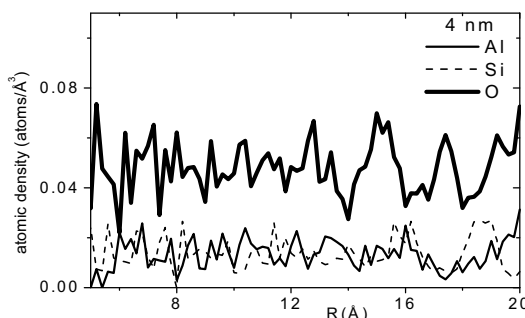


Fig. 4: Atomic density profile in amorphous AS₂ nanoparticle at 350 K.

Finally, we would like to show the thermodynamics quantities of amorphous AS₂ nanoparticles. Our calculations show that E_{pot} for nanoparticles, i.e. the potential energy of the systems, is significantly higher than that for the bulk one due to the surface energy of the formers. Thus, we can suggest the relation:

$E_{pot}^{nano} - E_{pot}^{bulk} = E_s$. Here, E_s is the surface energy of nanoparticles [19]. In present work, we have calculated the value for E_s only for the models obtained at 350 K after relaxation of 50000 MD steps. E_s is equal to 0.456 J.m⁻², 0.442 J.m⁻², 0.429 J.m⁻² for the size of 2 nm, 3nm and 4nm, respectively. It seems that E_s has a tendency to decrease with increasing nanoparticle sizes like those observed for amorphous TiO₂ nanoparticles [21]. Although there is no experimental and calculating data for surface energy of amorphous AS₂ nanoparticles to compare, one can consider that the calculated E_s has a reasonable value, which is close to those obtained by calculations for silica nanoclusters, which is 0.67 J.m⁻² [22].

4 CONCLUSIONS

Via calculations for structural quantities such as interatomic distances, PRDFs, coordination numbers and bond-angle distributions at 350 K for three different sizes, we found that the amorphous AS₂ nanoparticles have a slightly distorted tetrahedral network structure in which Si and Al are mainly surrounded by four oxygen atoms. However, these results are different from those observed in the bulk one. The discrepancy may be related to the higher concentration of under-coordinated Al atoms on the

surface of nanoparticles. Moreover, size effects on structure of amorphous AS₂ nanoparticles were shown via the increase of triclusters with increasing of nanoparticle size. We found that surface energy of AS₂ nanoparticles has reasonable value and is close to those for amorphous SiO₂ nanosized systems.

REFERENCES

- [1] E. Gavilan, T. Doussineau, A.E. Mansouri, M. Smaïhi, S. Balme and J.M. Janot, *Comp. Ren. Chimie* 8, 1946, 2004.
- [2] A. Sakamoto, F. Sato and S. Yamamoto, *J. Non-Cryst. Solid* 352, 514, 2006.
- [3] B. Doušová, T. Grygar, A. Martaus, L. Fuitová, D. Koloušek and V. Machovič, *J. Colloid and Interface Sci.* 302, 424, 2006.
- [4] Y. Liu, T.J. Pinnavaia, *J. Am. Chem. Soc.* 125, 2376, 2003.
- [5] K.S. Triantafyllidis, A.A. Lappas, I.A. Vasolos, Y. Liu, H. Wang and T.J. Pinnavaia, *Catalysis Today* 112, 33, 2006.
- [6] J. Leivo, M. Lindén, C.V. Teixeira, J. Puputti, J. Rosenholm, E. Levänen, T.A. Mäntylä, *J. Mater. Research* 21, 1279, 2006.
- [7] C. Zha and G.R. Atkins, *J. Sol-Gel Scien. and Tech.* 19, 741, 2000.
- [8] Y.F. Tang, Z.D. Ling, Y.N. Lu, A.D. Li, H.Q. Ling, Y.J. Wang and Q.Y. Shao, *Mater Chem. Phys.* 75, 256, 2002.
- [9] G.J. Kramer, A.J.M. de Man and R.A. van Saten, *J. Am. Chem. Soc.* 13, 6435, 1991.
- [10] S. Sen and R.E. Youngman, *J. Phys. Chem. B* 108, 7557, 2004.
- [11] S.H. Risbud, R.J. Kirkpatrick, A.P. Tagliavore and B. Montez, *J. Am. Ceram. Soc.* 70, C10, 1987.
- [12] M. Schmücker, H. Schneider, K.J.D. MacKenzie and M. Okuno, *J. Eur. Ceram. Soc.* 19, 99, 1999.
- [13] M. Benoit, S. Ispas and M.E. Tuckerman, *Phys. Rev. B* 64, 224205, 2001.
- [14] R.D. Shannon, *Acta Crystallogr. Sect. A* 32, 751, 1976.
- [15] V.V. Hoang, N.H. Hung and N.N. Linh, *Phys. Scr.* 74, 697, 2006.
- [16] V.V. Hoang, N.N. Linh and N.H. Hung, *Eur. Phys. J. Appl. Phys.* 37, 111, 2006.
- [17] A. Winkler, J. Horbach, W. Kob and K. Binder, *J. Chem. Phys.* 120, 384, 2004.
- [18] V.V. Hoang, *Phys. Rev. B* 70, 134204, 2004.
- [19] A. Roder, W. Kob and K. Binder, *J. Chem. Phys.* 114, 7602, 2001.
- [20] V.V. Hoang, D.K. Belashchenko, V.T. M. Thuan, *Physica B* 348, 249, 2004.
- [21] V.V. Hoang, H. Zung and N.H.B. Trong, *Eur. Phys. Journal D*, 2006 submitted for publication.
- [22] I.V. Schweigert, K.E.J. Lehtinen, M.J. Carrier, M.R. Zachariah, *Phys. Rev. B* 65, 235410, 2002.